J Vis (2010) 13:89–96
DOI 10.1007/s12650-009-0018-1

REGULAR PAPER

Zhe Cui · Kenji Kodama · Hiroyuki Oyama · Kuniyuki Kitagawa

Two-dimensional observation of excited atoms and ions and excitation temperature in inductively coupled plasma using newly developed four channel spectrovideo camera

Received: 19 November 2009 / Accepted: 26 November 2009 / Published online: 8 January 2010

Abstract A four-channel spectrovideo camera was developed and applied to the measurement of spatially and spectrally resolved profiles of atomic and ionic emission in an inductively coupled plasma (ICP). Spatial distributions of argon and chromium atoms and iron ions in ICP were visualized successfully. The excitation temperature profiles of argon, chromium, and iron in ICP were also successfully constructed on the basis of the two-line method. The excitation temperature profiles obtained with a monochromator and the spectrovideo camera were in fairly good agreement.

Keywords Inductively coupled plasma · Optical emission spectrometry · Two-line method · Image analysis

1 Introduction

Inductively coupled plasma (ICP) is one of the most popular plasma sources. ICPs have found widespread applications not only in analytical methods such as ICP atomic emission spectrometry (ICP-AES) and ICP mass spectrometry (ICP-MS) but also in various fields of manufacturing, such as chemical vapor deposition (CVD) and reactive ion etching (Hill 1998; Boumans 1987; Abe et al. 2008).

However, phenomena in ICPs are very complicated and have not been fully understood, particularly in conjunction with behaviors and temperatures of molecules and atoms. Therefore, a considerable number of researches have been conducted on temperature measurements for understanding phenomena in ICPs (Engelhard et al. 2008; Tognoni et al. 2007; Grotti et al. 2006; Borkowska-Burnecka et al. 2006; Sengoku and Wagatsuma 2006; Lehn et al. 2003; Sung and Lim 2003). In all these studies, temperature measurements were performed using a commercial ICP apparatus and a built-in spectrometer. Thus, the measurement methods were single-pointed in nature. It is important to measure two-dimensional (2D) distributions of chemical species and excitation temperatures, for understanding phenomena in ICPs. However, monitoring systems for this purpose have not yet been fully developed. In this study, we newly developed a four-channel spectrovideo camera and tested it by applying it to measurements of 2D distributions of some specific elements introduced into an ICP. We then performed calculations for deriving excitation temperature profiles of these elements.

Z. Cui
Department of Applied Chemistry, Nagoya University, Nagoya, Japan

K. Kodama (✉) · H. Oyama · K. Kitagawa
EcoTopia Science Institute, Nagoya University, Furo-cho, Chikusa-ku, Nagoya 464-8603, Japan
E-mail: echo@esi.nagoya-u.ac.jp
Tel.: +81-52-7893916
Fax: +81-52-7893910

2 Experimental

2.1 Instrumentation

Figure 1 shows the schematic diagram of the experimental setup used in this study. A conventional ICP system (ICPQ-1000, Shimadzu Corporation, Japan) was adopted as the test plasma source. The coolant, plasma, and carrier gases were supplied from a cylinder of ordinary grade Ar. Their flow rates were regulated at 15, 1.2, and 1.0 dm^3 min^{-1}, respectively. The solution uptake rate was approximately 0.7 cm^3 min^{-1}. The RF power supplied to the ICP was maintained at 1 kW throughout the experiment.

We have developed two high-speed CCD video cameras-SPECTRA-4 I.I. (with an image intensifier) and SPECTRA-4 (without an image intensifier). These two video cameras are capable of simultaneously dividing one image into four images through an internal optical system (Fig. 2). Converged light from the object is collimated by the collimator lens. The collimated light beam is then divided into four beams by a tetrahedral prism. Thereafter, the required wavelengths are selected through the interference filters placed in the beamlines. Finally, the four different wavelength beams are combined and focused onto the CCD or ICCD by the imaging lens. As shown in Fig. 1, the camera is capable of taking pictures at four different wavelengths simultaneously. The images obtained with the video camera reflect the emission spectral intensity profiles at four different wavelengths in the plasma. In this study, the images were captured at a frame rate of 30 s^{-1}, and the 30 images were time-averaged. The excitation temperatures were estimated using the well-known two-line method.

Prior to observation with the spectrovideo camera, suitable wavelengths for measurements were determined. For this purpose and for comparison of excitation temperatures, a monochromator (MD-25T, JASCO Corporation, Japan) with a liner CCD multichannel detector was used and the emission spectra of Ar, Fe, Cr, and the background emission were measured at a height between 3 and 18 mm above the ICP torch head at intervals of 5 mm.

2.2 Procedures

The net spectral emission intensities were estimated after several series of emission lines were measured and background subtraction made with the monochromator. The excitation temperatures were calculated from the net spectral intensities on the basis of the Boltzmann plot. A Boltzmann plot is extensively used to measure the excitation temperature to obtain information about the excitation of emission, because it is not necessary to estimate the absolute emission intensity and to know the concentration of emitting species (Boumans 1987). The Ar atomic emission lines used for the Boltzmann plot are listed in Table 1. The *gA* value is a product of the statistical weight and the Einstein-A coefficient.

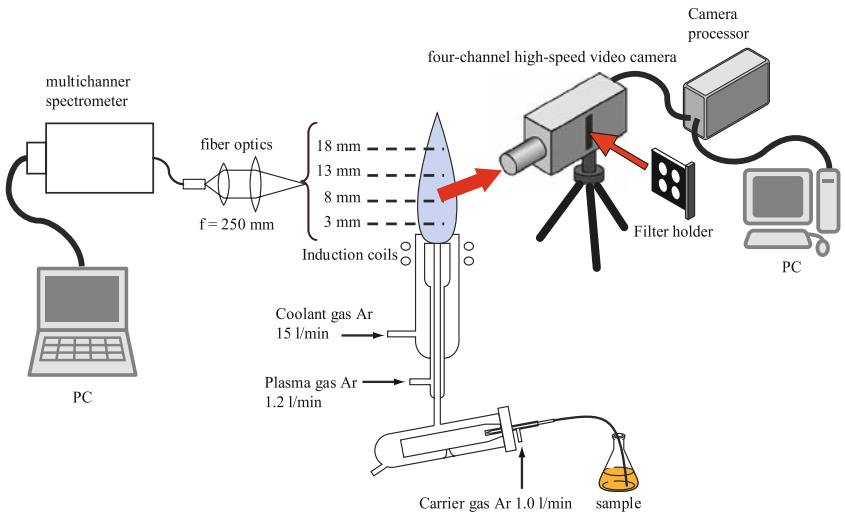

Fig. 1 Schematic diagram of experimental setup

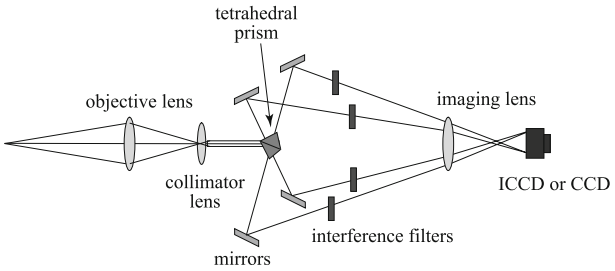

Fig. 2 Schematic diagram of optical setup of SPECTRA-4 I.I. and SPECTRA-4

Table 1 Argon atomic emission lines used for the Boltzmann plot

Wavelength (nm)	Upper level	eV	Lower level	eV	gA value $\times 10^8$
750.39	$3p^5(^2P_{1/2})4p^2[1/2]_0$	13.48	$3p^5(^2P_{1/2})4s^2[1/2]_1$	11.83	0.157
751.47	$3p^5(^2P_{3/2})4p^2[1/2]_0$	13.40	$3p^5(^2P_{3/2})4s^2[3/2]_1$	11.62	0.143
763.51	$3p^5(^2P_{3/2})4p^2[3/2]_2$	13.17	$3p^5(^2P_{3/2})4s^2[3/2]_2$	11.55	0.274
800.62	$3p^5(^2P_{3/2})4p^2[3/2]_2$	13.17	$3p^5(^2P_{3/2})4s^2[3/2]_1$	11.62	0.078
801.48	$3p^5(^2P_{3/2})4p^2[5/2]_2$	13.09	$3p^5(^2P_{3/2})4s^2[3/2]_2$	11.55	0.096
810.37	$3p^5(^2P_{3/2})4p^2[3/2]_1$	13.15	$3p^5(^2P_{3/2})4s^2[3/2]_1$	11.62	0.277
811.53	$3p^5(^2P_{3/2})4p^2[5/2]_3$	13.07	$3p^5(^2P_{3/2})4s^2[3/2]_2$	11.55	0.512

Table 2 Observed chemical species and specifications of their corresponding filters

Chemical species (wavelength, nm)	Center wavelength of filter (nm)	Half bandwidth of filter (nm)	Transmission (%)
Ar atom (750.39)	750.0	10	45
Ar atom (852.14)	850	10	45
Cr atom (357.87, 359.35, 360.53)	360.9	10.7	33.5
Cr atom (429.20, 430.05, 430.12)	431.4	10.7	51.6
Fe ion (256.25)	256.2	1.37	6.04
Fe ion (258.59)	258.8	1.44	6.96
Background (Fe)	265.8	1.75	8.87
Background (Fe)	267.2	1.68	9.25

Alongside, the profiles of the excitation temperature were calculated with the two-line method using the images observed with the spectrovideo camera, again after 2D background subtraction. The chemical species (elements) adopted for the two-line method are listed in Table 2, together with the center wavelengths, half bandwidths, and transmissions of the optical narrow bandpass filters. The SPECTRA-4 camera without the intensifier was used to obtain the images of atomic emission lines of Ar and Cr. However, because of very low transmission of optical filters for Fe ions and its background, SPECTRA-4 I.I. with the intensifier was used to obtain the images of Fe ions. All parameters used in the calculations were cited from Refs. Herrmann et al. (1963) and Boumans (1987).

2.3 Reagents

Sample solutions of 10 g dm^{-3} chromium and 5 g dm^{-3} iron were prepared by dissolving potassium chromate and ferric chloride of analytical grade in deionized water, separately.

3 Results and discussion

3.1 Correction for vignetting effect

The video cameras, SPECTRA-4 and SPECTRA-4 I.I., are capable of simultaneously taking four pictures at different wavelengths. However, these four pictures show the vignetting effect caused by the image dividing

optical system and interference filters. In order to correct this vignetting effect, four images of a white paper illuminated uniformly by an overhead projector were taken simultaneously. Figure 3a, b shows the vignetting effects when pictures were taken with SPECTRA-4 and SPECTRA-4 I.I., respectively. Each pixel in these figures is normalized to the maximum intensity. Throughout the subsequent measurements, emission spectral intensity profiles were obtained by dividing the raw profile by that shown in Fig. 3a or b, to give the correction for the vignetting effect.

3.2 Spatial distribution of emission intensity

The 2D emission intensity distribution of the elements in the plasma was constructed using the images obtained with the spectrovideo cameras.

In Fig. 4, the three images (a, b, and c) on the left are the emission spectral intensity profiles of the elements observed in the study, i.e., Ar atom, Cr atom, and Fe ion, respectively. These three profiles were then combined into one to obtain the image shown in the right (Fig. 4d). This figure clearly shows that the abundance of each element has its localization in the plasma.

Figure 4a also demonstrates that Ar atoms are rich about the symmetrical axis near the induction coil. Figure 4b, c again clearly shows that the elements introduced into the plasma are first atomized in the downstream region of the plasma and are then ionized in the downstream region along with the plasma flow.

3.3 Determination of excitation temperature from Boltzmann plot

Figure 5 shows the Boltzmann plots of the Ar I lines obtained from the spectrometer data. In Fig. 5, I is the intensity of the emission line and λ is the wavelength. This figure shows that the ICP is approximately in local thermal equilibrium (LTE) for the Ar atomic excitation system. Here, the excitation temperatures can be estimated from the slope of their plots and work out to 12,000 ± 250 K at 3 mm, 7,500 ± 170 K at 8 mm, 5, 800 ± 120 K at 13 mm, and 5, 100 ± 130 K at 18 mm, respectively.

3.4 Spatial distribution of temperature

3.4.1 Excitation temperature profile of Fe ions

Figure 6 shows images of spectral intensities of Fe ion lines and the background taken by SPECTRA-4 I.I. In this figure, strong emission from Fe ions was observed around the downstream region about the center axis. On the other hand, the background emission image shows the doughnut form about the symmetrical axis. Figure 7a shows the excitation temperature profile of Fe ions calculated with the two-line method

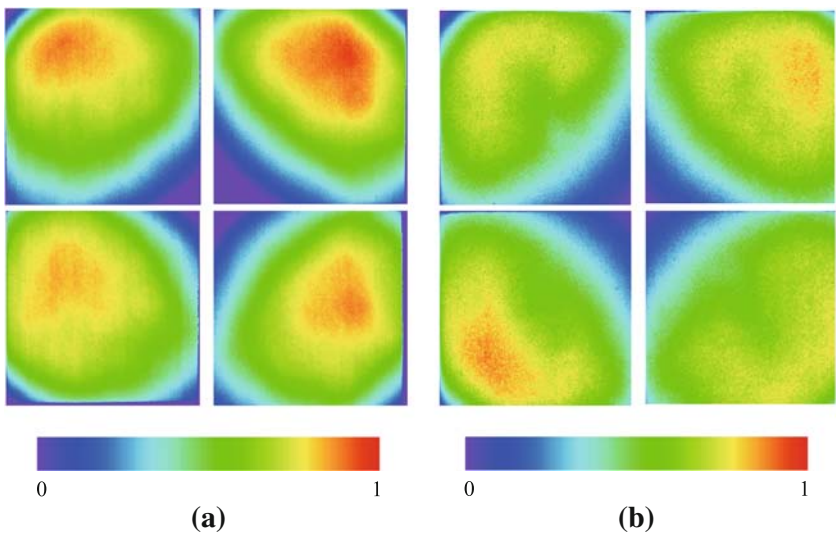

Fig. 3 Vignetting profile of **a** SPECTRA-4 and **b** SPECTRA-4 I.I

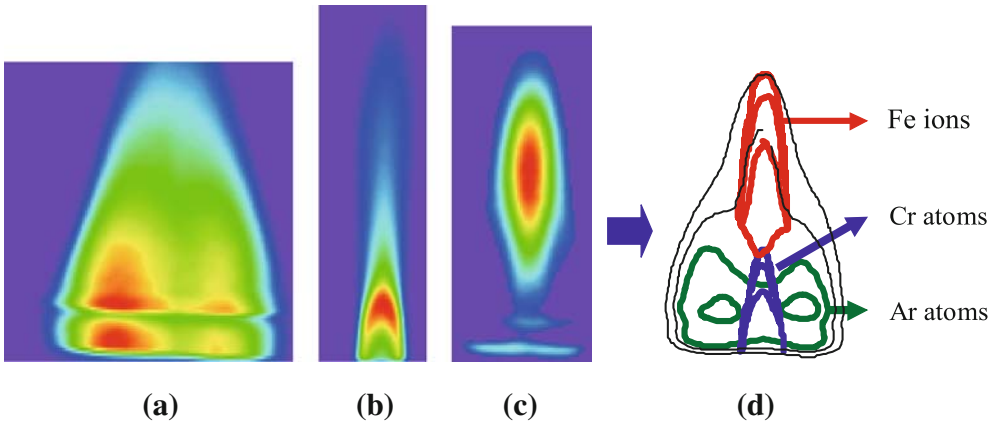

Fig. 4 Profiles of emission spectral intensity of some specific elements and their incorporation: **a** Ar atoms, **b** Cr atoms, and **c** Fe ions

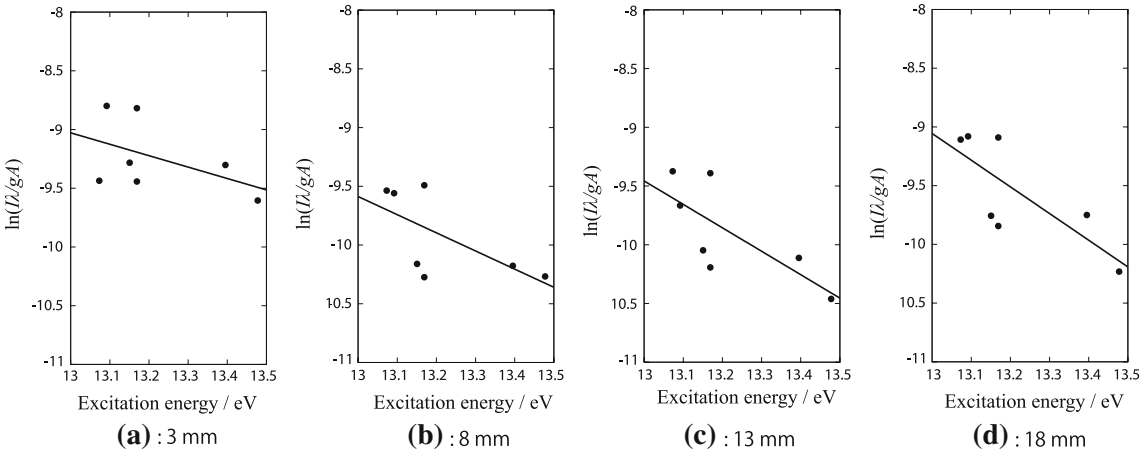

Fig. 5 Boltzmann plots of Ar atomic lines at observation heights of **a** 3 mm, **b** 8 mm, **c** 13 mm, and **d** 18 mm

using Fig. 6. It can be observed from Fig. 7a that the excitation temperature of Fe ranges between 8,000 and 16,000 K and that the profile area is limited to the downstream region of the plasma. The reason for the latter is that the number density of Fe ions is small in the upstream region of the plasma (Kitagawa and Holick 1992). Thus, the emission intensities of Fe ions in the upstream region of the plasma were too weak for the calculation of the excitation temperature.

3.4.2 Excitation temperature profile of Cr atoms

Figure 8 shows emission spectra of Cr atoms and Ar atoms in a range of 340–460 nm obtained with the monochromator. It can be noted that the Cr atomic emission lines overlap with the Ar atomic emission lines. In order to remove the background emission of the Ar lines, the Ar emission images were taken with SPECTRA-4 by spraying a blank solution, before the measurements with the Cr solution were performed.

Figure 9 shows the Cr emission and the background profiles. Because of the very high emission intensity from Cr atoms, these profiles were taken through an appropriate neutral density filter (1/8). Figure 7b shows the excitation temperature profile of Cr atoms calculated with the two-line method using the profile data shown in Fig. 9. The excitation temperature of Cr ranges between 4,000 and 6,000 K and increases downstream along with the plasma flow.

From the results shown in Figs. 6 and 9, it can be noted that the emission intensities of Fe ions and Cr atoms at the plasma edge are comparatively low, resulting in a sufficient signal-to-noise ratio. Thus, the excitation temperatures are not reliable at the plasma edge shown in Fig. 7.

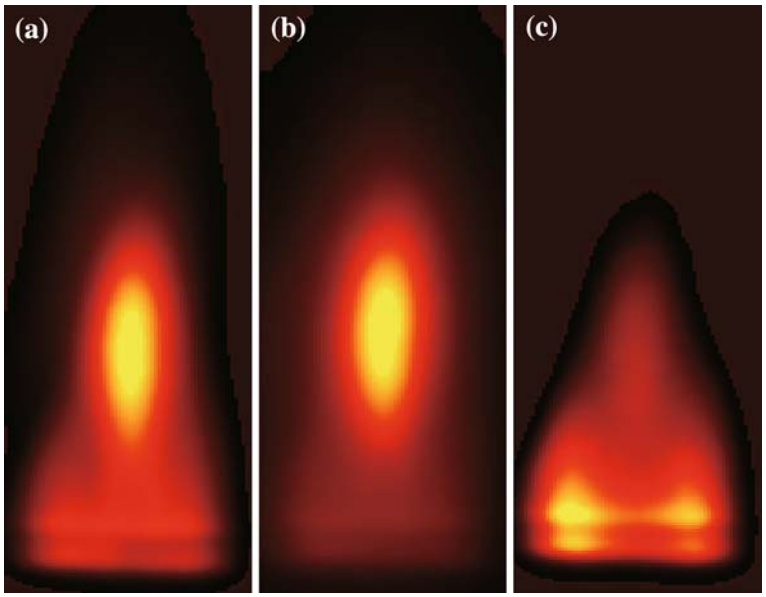

Fig. 6 Profiles of emission spectral intensity of Fe ions and background: **a** Fe ions 256 nm, **b** Fe ions 258 nm, and **c** background 267 nm

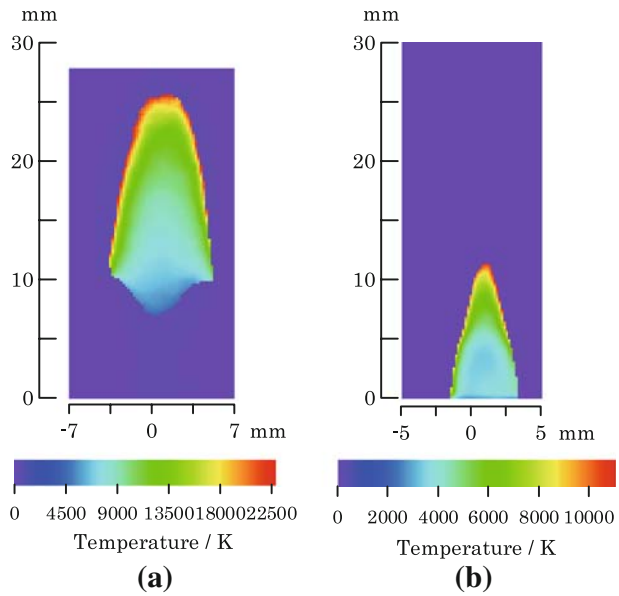

Fig. 7 Profile of excitation temperature of **a** Fe ions and **b** Cr atoms

3.4.3 Excitation temperature profile of Ar atom

Figure 10 shows the emission spectral intensities of Ar atoms taken by SPECTRA-4. These figures were corrected using the images shown in Fig. 3. The asymmetrical images reflect the fact that concentric symmetry of the plasma torch tube was not achieved during the glass blowing process. Figure 11 shows the excitation temperature profile of Ar atoms calculated with the two-line method using the data shown in Fig. 10. The excitation temperature of Ar ranges from 7,000 to 10,000 K. The high temperature zone exists in a toroidal form about the symmetrical axis of the plasma.

Figure 11 shows the comparison between the excitation temperature profiles of Ar atoms obtained with the monochromator and the spectrovideo camera. The figure indicates that these two profiles are in fairly

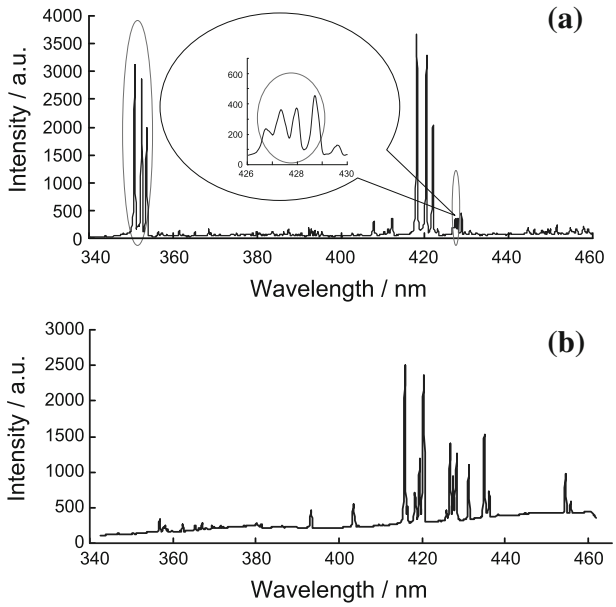

Fig. 8 Emission spectra of **a** Cr atoms and **b** Ar atoms

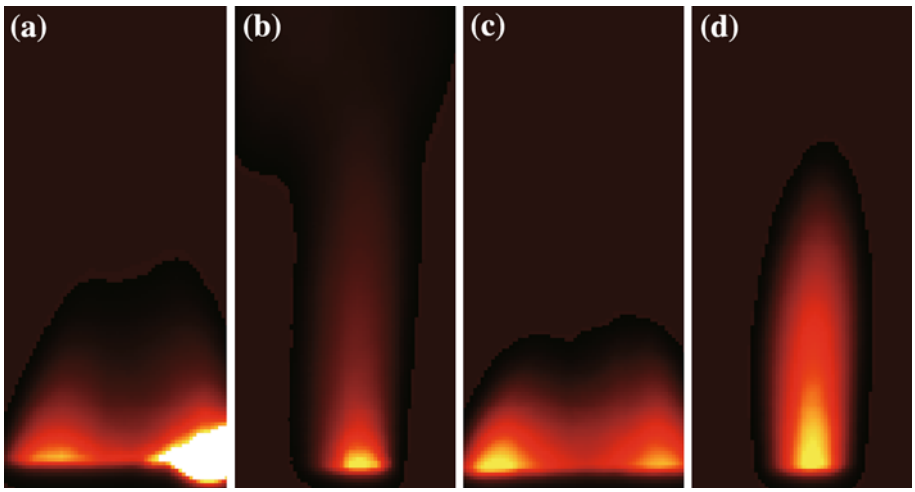

Fig. 9 Profiles of emission spectral intensity of Cr atoms plus background: **a** background 430 nm, **b** Cr atoms 430 nm, **c** background 360 nm, and **d** Cr atoms 360 nm

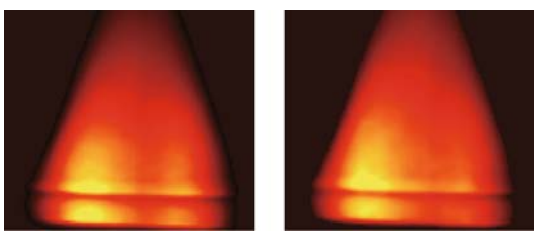

Fig. 10 Profiles of emission spectral intensity of Ar atoms: **a** Ar atoms 750 nm and **b** Ar atoms 850 nm

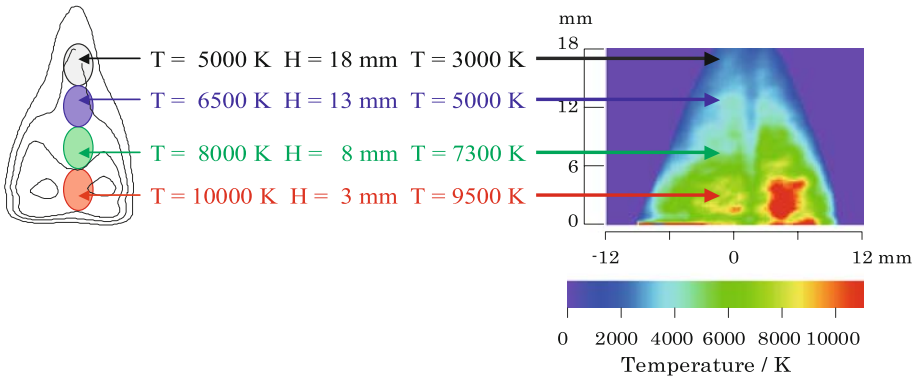

Fig. 11 Comparison between excitation temperature profiles of Ar atoms obtained with monochromator (*left*) and those obtained with high-speed video camera (*right*)

good agreement. Similarly, the two different temperature results for Fe ions in the plasma, except for those in the peripheral part of the plasma, are in satisfactory agreement.

4 Conclusion

The present study can be summarized as follows:

- Four-channel high speed spectrovideo cameras were successfully developed.
- 2D visualization of the excitation temperatures of argon, chromium, and iron was successfully carried out. A fairly good agreement was obtained between the results obtained with the developed spectrovideo camera and those with the conventional spectrometer.
- 2D visualization of argon and chromium atoms and iron ions in plasma was successfully carried out.

A further study for acquiring information on time-resolved images is currently under way.

References

Abe H, Yoneda M, Fujiwara N (2008) Developments of plasma etching technology for fabricating semiconductor devices. Jpn J Appl Phys 47:1435–1455. doi:10.1143/JJAP.47.1435

Borkowska-Burnecka J, Lesniewicz A, Zymicki W (2006) Comparison of pneumatic and ultrasonic nebulizations in inductively coupled plasma atomic emission spectrometry—matrix effects and plasma parameters. Spectrochim Acta B 61:579–587.doi:10.1016/j.sab.2006.04.005

Boumans PWJM (ed) (1987) Inductively coupled plasma emission spectroscopy part 1 and 2. Wiley, New York

Engelhard C, Chan GCY, Gamez G, Buscher W, Hieftje GM (2008) Plasma diagnostic on a low-flow plasma for inductively coupled plasma optical emission spectrometry. Spectrochim Acta B 63:619–629. doi:10.1016/j.sab.2008.03.015

Grotti M, Lagomarsino C, Mermet JM (2006) Effect of operating conditions on excitation temperature and electron number density in axially-viewed ICP-OES with introduction of vapours or aerosols. J Anal At Spectrom 21:963–969. doi:10.1039/b602162j

Herrmann R, Alkemade CTJ, Gilbert, Jr P (1963) Chemical analysis by flame photometry. Interscience Publishers, New York

Hill SJ (ed) (1998) Inductively coupled plasma spectrometry and its application. Sheffield Academic Press, Sheffield

Kitagawa K, Holick G (1992) Deviation of the level populations of iron atoms and ions from the boltzmann distribution in an inductively coupled plasma. Part 1. Spatial and power dependences. J Anal At Spectrom 7:1207–1219. doi:10.1039/JA9920701207

Lehn S, Huang M, Wamer K, Gamez G, Hieftje G (2003) Spatially resolved ground-state number densities of calcium and strontium ion in an inductively coupled plasma in contact with an inductively coupled plasma mass spectrometry sampling interface. Spectrochim Acta B 58:1647–1662. doi:10.1016/S0584-8547(03)00140-X

Sengoku S, Wagatsuma K (2006) Comparative studies of spectrochemical characteristics between axial and radial observations in inductively coupled plasma optical emission spectrometry. Anal Sci 22:245–248. doi:10.2116/analsci.22.245

Sung Y, Lim H (2003) Plasma temperature measurement of a low-pressure inductively coupled plasma using spectroscopic methods. J Anal At Spectrom 18:897–901. doi:10.1039/b303191h

Tognoni E, Hidalgo A, Canals A, Cristoforetti G, Legnaioli S, Salvetti A, Palleschi V (2007) Combination of the ionic-to-atomic line intensity ratios from two test elements for the diagnostic of plasma temperature and electron number density in inductively coupled plasma atomic emission spectroscopy. Spectrochim Acta B 62:435–443. doi:10.1016/j.sab.2007.05.006